

INTERNATIONAL SOCIETY FOR SOIL MECHANICS AND GEOTECHNICAL ENGINEERING



This paper was downloaded from the Online Library of the International Society for Soil Mechanics and Geotechnical Engineering (ISSMGE). The library is available here:

<https://www.issmge.org/publications/online-library>

This is an open-access database that archives thousands of papers published under the Auspices of the ISSMGE and maintained by the Innovation and Development Committee of ISSMGE.

Road construction on a soft organic subsoil

Construction d'une route sur un sol organique mou

I.Herle – *Institute of Theoretical and Applied Mechanics, Czech Academy of Sciences*

V.Herle – *SG-Geotechnika, Geologická 4, 15000 Praha 5, Czech Republic*

ABSTRACT: The design and the construction of a service road to the building site of a new bridge in Western Bohemia are described. The extremely soft organic subsoil (peat) reaches a maximum depth of almost 4 m at the construction site. Thus, based on in situ investigations and laboratory experiments, it was decided to put a cushion of crushed gravel in a reinforcement geotextile as a subgrade below the construction layers of the road. The cushion was placed directly on the ground surface since it was not possible to access the area with any vehicles prior to the soil improvement. A continuous monitoring of the surface deformation with horizontal inclinometers revealed settlements exceeding 90 cm. More than a half of this value was reached after the road construction. The maximum measured settlement was substantially higher than the initial prediction. Therefore a numerical analysis with finite elements was used in order to explain the difference.

RESUME: L'étude et la construction d'une route d'accès au chantier d'un nouveau pont sur une autoroute en Bohême de l'ouest sont évoqués ci dessous. Sur le chantier, le sous sol organique extrêmement mou (tourbe) atteint une profondeur de presque 4 m. Ses caractéristiques mécaniques ont été étudiées par essais sur place et en laboratoire. Comme support de construction pour la route, la solution proposée a été la création d'une couche de gravier concassé enveloppé par un géotextile de haute résistance en traction. La couche renforcée a été placée directement sur la surface du terrain. De par le fait que aucun véhicule ne peut accéder au chantier avant la mise en place du géotextile. La surveillance (monitoring) continu(e) du tassement en surface par inclinomètre horizontal a enregistré un tassement excédent 90 cm. Plus de la moitié du tassement mesuré s'est manifesté une fois la construction de la route terminée. Le tassement mesuré a été de beaucoup supérieur aux prévisions. Une analyse numérique par les éléments finis a été utilisée pour expliquer la différence.

1 INTRODUCTION

A new temporary service road has been built during the construction of the motorway bridge on the Radbuza near the city of Plzeň, Western Bohemia. A non-standard approach was needed due to the extremely soft organic subsoil (peat) reaching down to the maximum depth of 3.80 m. Below this soft layer alluvial deposits of medium dense sand formed a practically incompressible bottom layer.

Although the planed embankment reached the maximum height of only 1.4 m, a geotextile reinforcement was proposed. The geotextile was intended to inhibit pushing of the embankment material into the subsoil and to prevent the excessive lateral spreading of the embankment.

2 SOIL INVESTIGATIONS

Several in situ and laboratory investigations of the subsoil were done prior to the design of the embankment.

Shallow test pits revealed that below a thin stiff earth crust (about 0.2 m) there is a thick layer of organic soil (peat) with rests of plants. The groundwater level was found at 1.1 m below the ground surface.

With help of a light dynamic penetration using a 10 kg ram it was possible to locate the maximum depth of the soft layer equal to 3.8 m. The cone resistance in the soft layer remained in the range between 0.2 and 0.4 MPa (compared with the earth crust: 2 to 4 MPa). Below the soft layer a layer of a stiff alluvial deposit (medium dense sand, more than 10 MPa) represented an almost incompressible boundary.

Undrained cohesion $c_u \approx 23$ kPa was determined from field vane tests in the depths between 0.6 and 1.3 m. Even lower values of $c_u \approx 12$ kPa were obtained from laboratory

vane tests on undisturbed samples from the depth 1.2 m. A similar value $c_u = 10$ kPa was measured in unconsolidated undrained triaxial tests.

Soil compressibility was investigated in standard oedometer tests. The oedometric modulus E_{oed} ranged from 0.13 MPa at $\sigma_v = 20$ kPa to 0.20 MPa at $\sigma_v = 40$ kPa.

The drained shear strength was measured in a series of isotropically consolidated undrained triaxial tests (at $\sigma_r = 10, 30, 50$ kPa): $\varphi = 27^\circ$, $c = 6$ kPa.

3 ROAD CONSTRUCTION

The sequence of the construction of the embankment and of the road can be well described with help of photographs (Figures 1-3).

The geotextile GEOLON PP 500/40 was placed directly on the ground without removing the grass (Figure 1). This was necessary because of the low shear strength and high compressibility of the peat layer. The grassy crust enabled walking on the ground and laying of the geotextile sheets but it was impossible to approach the area with vehicles.

The first embankment layer of 0.4 m thickness was dumped on the geotextile and spreaded with a bulldozer without compaction (Figures 1 and 2). The geotextile sheets were then folded over the top of this layer (Figure 3).

Further layers of crushed gravel were placed on the geotextile cushion reaching the embankment height 1.4 m at the end of the construction. However, due to large settlements already during the construction stage (Figure 4) the total thickness of the embankment reached 1.85 m. Settlements measured by a horizontal inclinometer beneath the embankment show a continuous increase of the vertical deformation after the end of the construction approximately during one year, see Figure 4. A slight heave of



Figure 1: Geotextile placement on the grass and spreading of the gravel with a bulldozer.



Figure 2: Dumping of the crushed gravel on the geotextile.



Figure 3: Geotextile sheets folded over the first embankment layer.

the ground after another year depicts the unloading due to the removing of the most of the fill after the service period of the road. The nonsymmetric settlement profile can be either due to the inhomogeneous subsoil (varying layer thickness) or due to the insufficient measuring distance from the embankment axis on the left side.

4 NUMERICAL ANALYSES

Calculations presented in the sequel take into account only the overall behaviour of the embankment. The design of the reinforcement can be found elsewhere (Herle 1997).

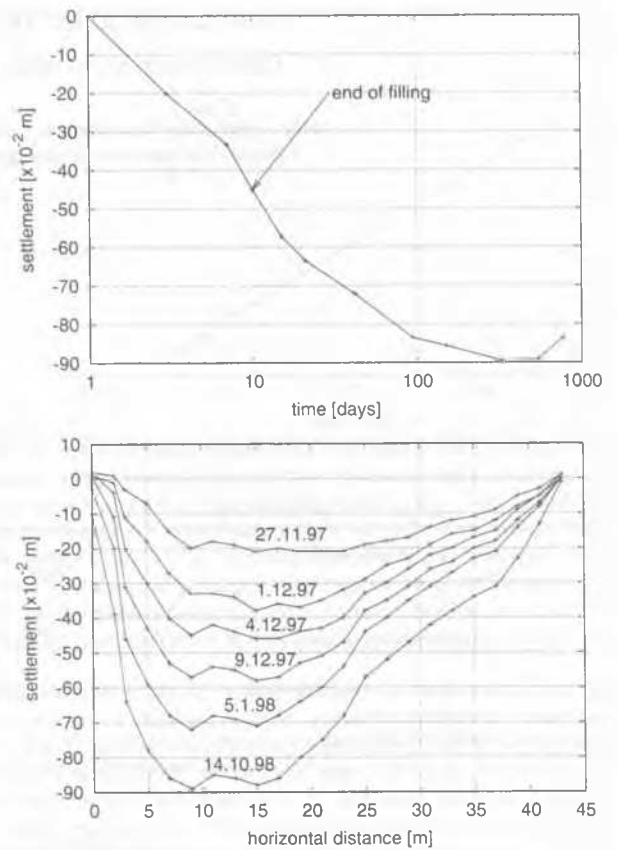


Figure 4: Measured settlements beneath the embankment at the embankment axis and settlement profiles at different times.

4.1 Preliminary estimations

During the design of the embankment its short-term stability was considered. According to the simplified bearing capacity equation

$$q_{max} = (2 + \pi)c_u \quad (1)$$

it could be expected that the maximum load q_{max} should not exceed 50 or 100 kPa, respectively. For the unit weight of the crushed gravel 2.0 t/m^3 the maximum height of the construction layer was limited to 0.25 or 0.5 m, respectively. It was assumed that the permeability of the organic layer is high enough and the generated excess pore pressures can sufficiently dissipate during the construction time of each embankment layer (such an assumption could be justified only due to the lower importance of the temporary structure).

From the back analysis of the continuous measurement of the settlement (Figure 4) it can be seen that 50% of the maximum settlement was reached at the end of filling, i.e. in 10 days. Thus, the consolidation coefficient c_v could be estimated as

$$c_v = \frac{z^2 T}{t} \approx \frac{(3.8/2)^2 \times 0.2}{10} = 0.072 \text{ m}^2/\text{d} \approx 10^{-6} \text{ m}^2/\text{s}. \quad (2)$$

This value is close to other values reported in the literature for similar peaty soils (Kogure 1999, Matsuda et al. 1999).

An estimation of the maximum settlement was important for the design of the embankment volume. Nevertheless, during the design stage it was not possible to perform a detailed numerical analysis and thus only a compression corresponding to the oedometric conditions was calculated:

$$s_{max} = \frac{h \gamma z}{E} \approx \frac{1.85 \times 20. \times 3.6}{200.} = 0.666 \text{ m} \quad (3)$$

The oedometric modulus of the soft layer $E = 0.2 \text{ MPa}$ was judged to be conservative enough for the average vertical effective stress in the middle of the soft layer:

$$\begin{aligned} \sigma_v &= \gamma_1 h + \gamma_2 z/2 + \gamma_3 d = \\ &= 20. \times 1.85 + 10. \times 3.6/2 + 0.2 \times 15 = 58 \text{ kPa} \end{aligned} \quad (4)$$

($\gamma_1 \dots$ embankment, $\gamma_2 \dots$ peat, $\gamma_3 \dots$ crust). Moreover, in situ conditions departing from the oedometric stress distribution and the high stiffness of the embankment compared to the soft subsoil were assumed to further diminish the calculated value of s_{max} .

A continuous measuring of the vertical deformation beneath the embankment showed, however, that the estimated value of s_{max} was surpassed by almost 50% and the maximum settlement reached 0.9 m. Thus, a FE analysis was performed in order to explain the difference.

4.2 FE simulation

It may seem that the finite element analysis of the above described problem is straightforward. However, many questions arise if looking into details.

In the sequel, all calculations were performed with a general-purpose FE code TOCHNOG which is available under the GNU public license (see <http://tochnog.sourceforge.net>). The finite element mesh was composed of linear triangle and quadrilateral elements. Due to the linearity of elements, a very dense mesh was assembled. An implicit integration of the state variables was performed.

A short term stability of the embankment is often important during the construction. It was already shown in the preceding section that the embankment stability may be violated in this case. Moreover, a fully undrained analysis (using undrained cohesion c_v) need not be sufficient and need not capture the most dangerous states. In order to judge the overall situation, a coupled analysis is needed which takes into account a simultaneous generation and dissipation of pore pressures. Unfortunately, an additional necessary soil parameter (permeability) was not measured and could be but estimated. Therefore, the coupled calculation is not considered in this paper and the presented analysis concentrates on the long-term settlement prediction.

The mechanical behaviour of soils is usually described with an elastic-perfectly plastic Mohr-Coulomb model for practical purposes. Consequently, the soil remains elastic inside the limit stress envelope and plastic strains are generated only at the maximum shear stresses. Such a model can be used only for monotonic loading when unloading/reloading cycles need not be taken into account. The list of the subsoil parameters for this case is given in Tab. 1.

There are several possible approaches how to simulate numerically the settlement induced by loading due to the embankment construction (Figure 5). It will be shown in the following sections that the scatter of the obtained numerical results can be very large.

Table 1: Parameters of the subsoil used in FE calculations.

Layer	E [MPa]	ν [-]	φ [°]	c [MPa]	ψ [°]	γ [t/m ³]
Crust	20.	0.3	27.	0.025	0.	1.5
Peat	0.2	0.1	27.	0.006	0.	1.0
Sand	20.	0.3	35.	0.001	10.	1.7

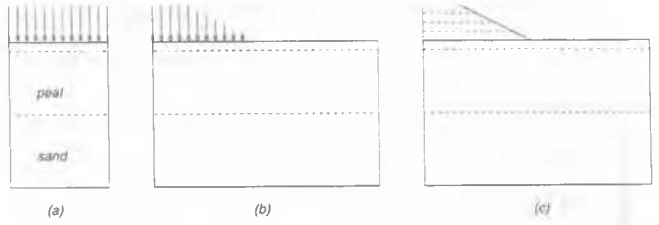


Figure 5: Possible approaches to the numerical modelling of the embankment settlement.

4.3 Oedometric conditions

One can start with quasi-oedometric conditions in order to check the numerical model and to compare it with analytical calculation (Figure 5a). The calculated settlement is uniform in this case and the value 0.65 m agrees with the initial estimate. However, this value was obtained using the common *small strain* approach which is rather questionable for such large settlements (vertical strains reach 18%).

The *Updated Lagrange* method results in so-called logarithmic strains producing the maximum settlement 0.51 m. Thus, the difference in results of both methods even for linear elasticity exceeds 20%.

Another uncertainty related to the calculation is due to the material model. A constant value of the elastic modulus E does not respect the results of laboratory experiments showing an increase of E with increasing stress. A power-law model in form

$$E = E_0 (\sigma/\sigma_0)^n \quad (5)$$

would be more appropriate. This relation was already proposed by Ohde in the thirties (for $n = 1$ it results in the Terzaghi semilogarithmic compression law) and it is a part of several more advanced constitutive models. Inserting the measured values of E for corresponding values of σ , one obtains $n \approx 0.6$. The application of the power-law model in the Updated Lagrange framework yields the settlement 1.02 m. In spite of a slight overprediction, this value is rather close to the measured one.

4.4 Trapezoidal loading

The trapezoidal load distribution (Figure 5b) resembles more the loading situation in the field. It corresponds to the embankment with zero stiffness. The calculated settlement is no more uniform and purely vertical. Oedometric conditions can be assumed only close to the embankment symmetry axis. In order to avoid tensile strains at the inflex point of the settlement profile, no tensile stresses were allowed even in the elastic calculations.

Maximum values of the settlement are similar to the oedometric case but the settlement distribution becomes bell-shaped (Figure 6). The plastic calculation produces almost twice as high settlements as the elastic one. This is the consequence of the pronounced lateral spreading of the soil beneath the embankment in case of plastic deformation. Furthermore, the settlement profile changes distinctly and the maximum settlement is not reached at the symmetry axis. This effect can be observed in the field measurements (Figure 4) as well.

4.5 Comprehensive analysis

Including the construction of the embankment into the numerical simulation (Figure 5c) can be considered as the most appropriate (but the most difficult) strategy. Additionally to

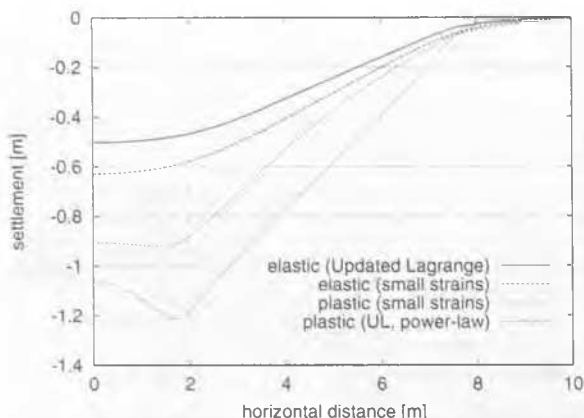


Figure 6: Settlement distribution in case of the trapezoidal surface load.

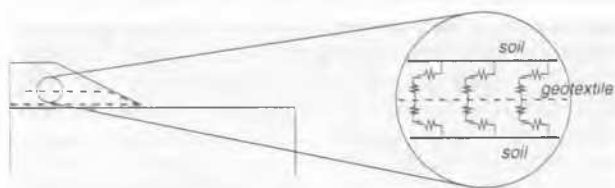


Figure 7: Simulation of the geotextile.

the already discussed problems one must take into account the interface behaviour between soil and geotextile.

When performing a FE calculation with such a model, even embankment layers without geotextile work as a reinforcement since the elastic stiffness allows large tensile stresses within the embankment. Thus, tensile stresses in the soil must be prohibited in the calculation.

Within the TOCHNOG code, *trussbeam* elements with zero compressive forces and zero bending stiffness were applied for the modelling of the geotextile (Figure 7). The yield stress $\sigma_y = 50$ MPa and the elastic modulus $E_g = 500$ MPa were derived from the tensile strength 500 kN/m being reached at 10% elongation (for the thickness of the geotextile 0.01 m). Interface behaviour between soil and geotextile was assumed to be perfectly plastic governed by the angle of internal friction 10° (geotextile-subsoil) and 25° (geotextile-embankment), respectively. Thus, a different friction along two opposite sides of one geotextile was prescribed. *Contactspring* elements worked as interface elements in the calculations.

The loading process due to the embankment filling resulted from a gradual increase of the material density with calculation time. The crushed gravel from the embankment was considered elastic ($E=50$ MPa, $\nu=0.2$) with no tension stresses allowed. The subsoil was described with elastoplastic model (power-law elasticity) in the Updated Lagrange framework.

The simulation results in Figure 8 show a different settlement profile than in case of the trapezoidal load. The maximum settlement is smaller but it is distributed over a wider area. This can be explained by a stiffer contact between the subsoil and the embankment due to the geotextile cushion.

5 CONCLUSIONS

The case study of the embankment on a very compressible peaty soil shows difficulties related to the prediction of settlements. There are several engineering approaches possible which yield different results. The numerical analysis should

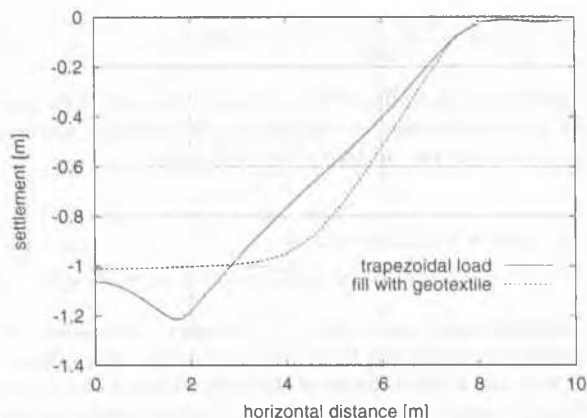


Figure 8: Settlement distribution with and without the geotextile cushion.

therefore respect in a maximum possible way laboratory experiments. The decisive role plays the nonlinearity of the soil behaviour which can be captured by a stress-dependent elasticity modulus. Including the limit shear stresses (perfect plasticity) enables to reproduce a realistic shape of the settlement profile at the surface.

The results of numerical simulations coincide well with the in situ measurements. Nevertheless, the applied approach can predict only maximum settlements disregarding the short-term stability. A more comprehensive analysis of the problem should also involve time effects (coupled consolidation and creep).

ACKNOWLEDGEMENT

The support by the Grants No. 103/99/P005 of the Grant Agency of the Czech Republic and No. COST C7.50 of the Czech Ministry of Education is gratefully acknowledged.

REFERENCES

- Herle, V. 1997. Radbuza — geotechnical investigation and design of the temporary roads. *Report SG-Geotechnika*.
- Kogure, K. 1999. Consolidation and settlement of peat under loading. In E. Yanagisawa, N. Moroto & T. Mitachi (eds.), *Problematic soils*: 817–832. Rotterdam: Balkema.
- Matsuda, H., S. Kobayashi, Y. Sutoh & Y. Itadani 1999. Engineering properties of organic soil for the ground improvement. In E. Yanagisawa, N. Moroto & T. Mitachi (eds.), *Problematic soils*: 15–19. Rotterdam: Balkema.